Bioengineered human myobundles mimic clinical responses of skeletal muscle to drugs

Lauran Madden, Mark Juhas, William E Kraus, George A Truskey, Nenad Bursac

DOI: http://dx.doi.org/10.7554/eLife.04885

Cite as: eLife 2015;10.7554/eLife.04885

Received: 23 September 2014
Accepted: 8 January 2015
Published: 9 January 2015

Bioengineered Human Myobundles Mimic Clinical Responses of Skeletal Muscle to Drugs

Lauran Madden[1], Mark Juhas[1], William E. Kraus[2], George A. Truskey[1], and Nenad Bursac[1]*

[1]Department of Biomedical Engineering, Duke University, Durham, NC

[2]Department of Medicine, Duke University School of Medicine, Durham, NC

***Corresponding author:**

Nenad Bursac, PhD

Rooney Family Associate Professor of Biomedical Engineering

Associate Professor of Medicine

Duke University

Room 136 Hudson Hall

Durham, NC 27708

Phone: 919-660-5510

Fax: 919-684-4488

Email: nbursac@duke.edu

Keywords: Tissue engineering, human skeletal muscle, contractile force, muscle physiology, drug testing

Abstract

Existing *in vitro* models of human skeletal muscle cannot recapitulate the organization and function of native muscle, limiting their use in physiological and pharmacological studies. Here, we demonstrate engineering of electrically and chemically responsive, contractile human muscle tissues ("myobundles") using primary myogenic cells. These biomimetic constructs exhibit aligned architecture, multinucleated and striated myofibers, and a $Pax7^+$ cell pool. They contract spontaneously and respond to electrical stimuli with twitch and tetanic contractions. Positive correlation between contractile force and GCaMP6-reported calcium responses enables non-invasive tracking of myobundle function and drug response. During culture, myobundles maintain functional acetylcholine receptors and structurally and functionally mature, evidenced by increased myofiber diameter and improved calcium handling and contractile strength. In response to diversely acting drugs, myobundles undergo dose-dependent hypertrophy or toxic myopathy similar to clinical outcomes. Human myobundles provide an enabling platform for predictive drug and toxicology screening and development of novel therapeutics for muscle-related disorders.

Impact Statement

A novel bioengineered human skeletal muscle model with accurate physiological and pharmacological responses may provide a useful tool for preclinical testing.

Introduction

Development of human *in vitro* systems for basic biological studies and drug discovery is motivated by the need to improve outcomes in human patients and alleviate ethical considerations demanding a reduction in the use of animals(1, 2). While significant progress has been made towards predictive *in vitro* models for liver, lung, and cardiac tissues(2), a functional model of human skeletal muscle has not been described. This is of particular concern as there

are a wide range of metabolic, neuromuscular, and dystrophic disorders involving skeletal muscle that are under investigation and still lacking therapies. Skeletal muscle is also central to diseases with high societal impact and those that do not have adequate animal models, including diabetes, obesity, and different dystrophies. Furthermore, through secretion of contraction-dependent myokines, skeletal muscle has been strongly implicated in organ-organ interactions including processes as diverse as cognition, inflammation, cancer, and aging(3). The need for an accurate preclinical model of human skeletal muscle was exemplified by the market withdrawal of cerivastatin that was well tolerated in mice but caused fatal rhabdomyolysis in humans(4, 5).

Expansion of primary human myoblasts and formation of myotubes in two-dimensional (2D) systems is well known, however, these cultures are difficult to maintain over long times, lack the architecture of native muscle, and require complex media components to initiate spontaneous contractions(6-8). The contractile force of single, *in vitro* cultured human myofibers can be measured(9), though such a system is limited by its inability to investigate biochemical changes or cell-matrix interactions that can be critical in different pathologies including muscle dystrophies and wasting disorders(10). While three-dimensional (3D) culture models of rodent skeletal muscle have measureable contractile force(11-15) and can be applied to drug testing(15) and disease modeling(16), *in vitro* 3D systems using primary human myoblasts rely on measurements of passive force(17-19) which is not specific to functional skeletal muscle.

Here, we describe a biomimetic human skeletal muscle culture system ("myobundle") amenable to studies of contractile function and biochemical changes in response to a wide range of stimuli. Conditions for primary myogenic cell expansion and 3D tissue formation were optimized to reproducibly obtain contractile myobundles consisting of aligned, cross-striated myofibers and a pool of cells expressing the satellite cell marker Pax7. In response to electrical and pharmacological stimuli, myobundles exhibited forceful contractions and calcium transients which could be non-invasively measured to track physiological responses and functional

maturation over time. Reproducible functional characteristics were obtained using cells from nine different donors and one commercial source. Similar to clinical outcomes in humans, when pharmaceutically challenged, myobundles experienced enhanced contractile performance in response to a steroid-like substance, underwent autophagic myopathy following administration of an anti-malarial agent, and exhibited statin-induced weakness and lipid accumulation.

Results

Structure and Composition of Myobundles

Myogenic cells were isolated from human muscle biopsies and expanded for 3-5 passages, when they contained a significant fraction of muscle precursors positive for desmin and MyoD (Figure 1 – figure supplement 1). Engineered human skeletal muscle 'myobundles' were generated using a hydrogel molding technique (Figure 1*A,* Figure 1 – figure supplement 2) we developed for rodent cells(13, 14). Following hydrogel compaction for 3-5 days, low serum media was applied to induce myofiber formation and differentiation. After an additional 3-5 days, the myobundles began to spontaneously twitch (Video 1), which was previously reported only in rodent 3D muscle constructs(11). After two-week culture, the myobundles contained densely packed and aligned myofibers embedded in a laminin-rich matrix (Figure 1*B*) and surrounded at the periphery by vimentin^{+} fibroblasts (Figure 1 – figure supplement 3A-C). Mature structure of the myofibers was evident by the expression of myosin heavy chain (MYH), sarcomeric alpha-actinin (SAA) cross-striations, and multiple myogenin^{+} nuclei (Figures 1*C-E* and Figure 1- figure supplement 2*B-C*). Of functional importance, acetylcholine receptors, which are necessary for neuromuscular junction formation, were present at the myofiber surface (Figure 1*F*). While the majority of expanded myogenic cells fused to form myofibers, a fraction of cells continued to express the satellite cell marker Pax7 (Figure 1*G*), suggesting regenerative capacity as described in a rat culture model(14). With time in culture, structural maturation of myobundles was evident from the progressive increase in myofiber diameter (13.5 ±1.5 μm and 21.8 ± 2.8

μm at 1 and 4 weeks of culture, Figure 1*H*, Figure 1 – figure supplement 3*D*) and expression of the muscle-specific proteins (MYH, SAA, and muscle creatine kinase (MCK), Figure 1*I*), while myofiber length and myonuclei number (524±70 and 7±3.6, respectively, at 3 weeks of differentiation) remained relatively steady with time of culture (Figure 1 – figure supplement 4).

Contractile Force Generation of Myobundles

The amplitude of induced contractile force by electrical or chemical stimulation is a key parameter used to evaluate skeletal muscle function both *in vivo* and *ex vivo* on isolated muscle fibers (20, 21). To optimize contractile force output of myobundles, myogenic cells were expanded in media containing either bFGF(22) or EGF(23). Despite comparable myoblast purity and myofiber formation in 2D culture, myobundles made of EGF-expanded cells had superior contractile function (Figure 2 – figure supplement 1). In addition to spontaneous contractions, myobundles also contracted in response to electrical stimulation (Video 2) and, similar to native muscle(24), exhibited stronger contraction with an increase in stimulation frequency and myobundle length (Figure 2*A*-*B*, Figure 2 – figure supplement 2). In concert with observed structural maturation, amplitudes of twitch and tetanus force in myobundles increased over four weeks in culture (Figure 2*C*), while twitch kinetics remained unchanged (Figure 2*D*).

To evaluate the robustness of the developed methodology, we expanded and utilized cells from nine donor muscle samples (obtained by needle biopsy or surgical waste) and one commercially available myoblast source (Lonza). Expanded cells from all ten sources formed functional myobundles that contracted in response to electrical stimulation with an average specific force of 2.1 ± 0.9 mN/mm^2 and 7.0 ± 2.2 mN/mm^2 for twitch and tetanus, respectively (Figure 2*E*). The average tetanus force was similar to values measured in fetal human muscle(25) and an order of magnitude lower than values reported for adult muscle(25, 26), while average tetanus-to-twitch ratio (3.5 ± 0.8, Figure 2*E*) was within the normal adult range(26). The kinetic parameters of twitch contraction were also evaluated for each donor

sample (Figure 2*F*) and were on average two-fold slower than those of adult human muscle(21) and comparable to those of single *in vitro* cultured human myotubes(9).

Calcium Handling of Myobundles

To expand the utility of the myobundle platform, we incorporated a capability for non-invasive real-time monitoring of calcium transients in myobundles as calcium handling is critical to normal muscle function and can be affected by pathological conditions including dystrophic disorders and malignant hyperthermia(27). Expanded myogenic cells were lentivirally transduced with a calcium indicator, GCaMP6(28), driven by a muscle-specific promoter, MHCK7(29), prior to myobundle formation. As a result, robust expression of GCaMP6 in differentiated myofibers (Figure 3*A*) allowed detection of both spontaneous and electrically stimulated calcium transients in myobundles (Figure 3*B*, Video 3) under a variety of conditions. In response to 10 Hz (tetanic) vs. single (twitch) stimuli, the amplitude of calcium transients increased (Figure 3*C-D*), as measured by normalized change in fluorescence intensity (ΔF/F), similar to the increase in contractile force with tetanic stimulation. Additionally, with longer time in culture, calcium transient amplitude increased (Figure 3*D*) and correlated with the contractile force amplitude measured in the same bundles (Figure 3 – figure supplement 1).

We further tested the functionality of calcium-handling machinery in myobundles by biochemical stimulation with caffeine and acetylcholine (ACh). By opening of ryanodine receptors, caffeine is known to generate concentration-dependent calcium release and contraction in skeletal muscle (27, 30), as was observed in myobundles from different donors (Figure 3 – figure supplement 2, Video 4). ACh is released at the neuromuscular junction to stimulate muscle contraction via opening of ligand-gated Na/K-permeable channels and voltage-gated Ca channels, while ACh receptors are a target of different muscle relaxants and toxins(31). The degree of calcium release in response to a bolus of 10 mM ACh (Figure 3*E*, Video 5) was comparable to that from electrically stimulated tetanus (Figure 3F) and unchanged throughout the entire culture period (Figure 3 – figure supplement 3A). Tubocurarine, a muscle

relaxant, blocked ACh (but not electrically) induced calcium transients (Figure 3F) and contractions (Figure 3 – figure supplement 3*B-C*), mimicking the neuromuscular block observed *in vivo*(32).

Drug Testing of Myobundles

We evaluated the potential application of myobundles as a preclinical test bed by studying their responses to three classes of pharmaceutical agents with a broad range of known effects. Statins are widely prescribed to prevent coronary artery disease, however even at normal doses some of them can induce significant myopathic weakness and rhabdomyolysis after as early as two weeks of use(5, 33). We tested the effects of lovastatin and cerivastatin at their clinically-relevant dose ranges (100-fold higher for lovastatin due its lower bioavailability and bioactivity(34, 35)) encompassing both maximum therapeutic blood serum concentrations and higher doses known to accelerate myopathic induction(33). In our studies, 2-week application of each statin was well tolerated in the myobundles derived from two of three donors at their respective therapeutic doses, while higher doses induced significant contractile weakness in the myobundles from all donors (Figure 4*A-B*). Unlike human myobundles that replicated clinical response, murine engineered muscle tissues in previous studies exhibited a sharp decrease in contractile function even at the lowest statin dose tested(15). Human myobundles also recapitulated the histopathology of statin-associated myopathy characterized by dose-dependent lipid accumulation(5) (Figure 4*C*).

We also challenged myobundles with the anti-malarial agent chloroquine for one week to evaluate its effects on autophagy, a conserved lysosomal pathway in both physiological and pathological conditions(36). With increasing doses of chloroquine, myobundles from all donors exhibited a decrease in contractile force generation (Figure 4D), which was associated with the autophagic buildup marked by conversion of LC3B-I to LC3B-II and a decrease in the expression of the contractile protein SAA (Figure 4*E-F*). These outcomes were consistent with autophagic-related myopathy seen in humans treated with chloroquine(36, 37). Similar

biochemical responses to chloroquine including accumulation of LC3B-II and reduction of contractile proteins was also observed in 2D cultures (Figure 4 – figure supplement 1).

Clenbuterol is a β2-adrenergic agonist with both short and long-term concentration-dependent effects on muscle, improving contractile force and hypertrophy at low concentrations, while inducing apoptosis and necrosis at high concentrations(38). Clenbuterol and other β-agonists are under investigation for prevention of muscle wasting(39), however, species-dependent differences in their anabolic effects limit the usefulness of preclinical animal studies(40). In our studies, both acute and chronic application of clenbuterol induced an *in vivo*-like biphasic dose-dependent effect on contractile force generation of myobundles (Figure 4*G-H*) with the typical anabolic response and stronger contractions at 0.1 µM and diminished contractile response above 1 µM. The observed positive inotropic effect of 0.1 µM clenbuterol was partially attributed to myofiber hypertrophy (Figure 4I) and was confirmed in myobundles from multiple donors, resulting in an average force increase of 43.2 ±10.8% (Figure 4 – figure supplement 2). Collectively, these results confirm the functional similarity of myobundles to human muscle tissue and validate their potential use in the future predictive studies of muscle physiology.

DISCUSSION

We described the development and validation of the ‘myobundle‘, a biomimetic human skeletal muscle culture platform for clinically relevant *in vitro* studies of muscle physiology and drug development. Myobundles recapitulate key functional aspects of human skeletal muscle including a functioning contractile apparatus, responsive acetylcholine and β2-adrenergic receptors, and physiological calcium handling, all of which are involved in pharmacological side effects in humans(41). Long-term electrical and chemical responsiveness of myobundles allow for both acute and chronic physiological and pharmacological tests. Reproducibility and robustness of the system were demonstrated using biopsies from multiple donors and a commercial cell source. Correlated force generation and calcium transient responses recorded

via the use of genetically encoded calcium indicators(28) enabled continuous optical monitoring of the relationship between stimuli and functional effects, thus bridging a significant gap in current testing methods(1).

Existing methods to measure contractile function of human muscle *in vitro* rely on acute, single-time use of intact muscle fibers isolated from patient biopsies(20). While 2D and 3D cultures can be used to form *de novo* muscle fibers from human myogenic cells, existing methods fail to reproduce a comprehensive range of myofiber physiological responses, such as twitch, tetanus, and chemically induced contractions. Compared to previous 3D culture studies(18, 19), a relatively high cell density, specific hydrogel and media compositions, and dynamic culture conditions(42) used in our system may have all contributed to the robust formation of functional human engineered muscle. Under these conditions, the ability to generate large numbers (>1000) of contractile myobundles from a single donor biopsy allowed us to perform traditional physiological and biochemical measurements in both acute and chronic settings and for multiple testing compounds and conditions. Electrically induced calcium transients and contractions (twitch and tetanus) as well as physiological responses to increase in muscle length and stimulation frequency(24, 26) were reproducibly recorded in myobundles from ten donors. The specific blockade of acetylcholine-induced but not electrically-induced calcium release by the muscle relaxant and acetylcholine receptor blocker tubocurarine mimicked responses seen in human studies(32). Along with dose-dependent increase in calcium transient amplitude by caffeine, these experiments demonstrate that myofibers formed within the 3D myobundle culture environment exhibited intact excitation-contraction coupling and physiological responsiveness to both chemical and electrical stimuli. While repeated non-invasive interrogation of myobundle function was limited to calcium imaging, integration of smaller size myobundles with high-throughput force testing assays should be feasible as demonstrated for mouse cells(15).

The utility of myobundles as a preclinical drug testing platform was evaluated by measuring contractile and biochemical responses to statins, chloroquine, and clenbuterol. Statin myopathy is a common side effect that has been reported for all currently available statins(5, 33). Similar to clinical reports, human myobundles showed higher sensitivity to cerivastatin than lovastatin(34) and at excessive statin concentrations displayed progressive weakness and lipid accumulation, suggestive of equivalent mechanisms of action *in vitro* and *in vivo*. The use of myobundles allowed direct comparison of similar pharmaceuticals on the same patient or cohort, previously recommended for but unavailable for statins due to the variations among clinical trials and underreporting of symptoms(5, 33). In response to an anti-malarial agent, chloroquine, myobundles showed induction of autophagic myopathy also observed in native muscle(36), thus providing a potential functional screen for non-toxic modulators of autophagy. We also tested the acute and chronic responses of myobundles to β2-adrenergic agonist clenbuterol and observed myofiber hypertrophy and increased contractile strength at low clenbuterol doses followed by muscle weakness at higher doses, consistent with previous animal and human studies(39). Currently, binding affinity to β2-adrenergic receptors is one of the standard tests for drug specificity(41) and is also a potential target for therapies in muscle wasting disorders(39). Overall, these results suggest that myobundles closely mimic the functional responses of native human muscle through multiple signaling pathways and could provide a pre-clinical assay for predictive screening of novel therapeutics for a broad range of muscle-related disorders.

Our *in vitro* model of human skeletal muscle provides a tool for improved predictive pharmacological testing and a potential alternative to costly animal studies. Non-destructive, real-time measurement of function such as calcium handling shown here could be combined with other optically-based assays(43) to elucidate mechanisms of drug action. The ability to measure and quantify functional endpoints in myobundles in a population- or patient-specific manner allows construction of pharmacological time- and dose-response curves previously not

available for human skeletal muscle. The myobundles may be integrated with other established human micro-organ systems such as liver or heart for more predictive body-on-chip toxicology studies(2). Functional acetylcholine receptors within myobundles are integral to studies involving the neuromuscular junctions and necessary for potential implantation of such tissues to repair muscle dysfunction or loss. Eventual applications of myobundle platform using patient-derived cells to model functional deficits observed in different muscle pathologies may allow development of more efficacious therapies and safe translation to clinics.

MATERIALS AND METHODS

Preparation of Myogenic Cells

Human skeletal muscle samples were obtained through standard needle biopsy or surgical waste under Duke University IRB approved protocols. Nine donor samples were expanded by outgrowth similar to methods previously described(6). Briefly, muscle samples were minced, washed in PBS, and enzymatically digested in 0.05% trypsin for 30 minutes. Muscle was collected by centrifugation, pre-plated for 2 hours, and transferred to a matrigel (BD) coated flask for attachment. Cells were expanded in skeletal muscle growth media containing low glucose DMEM, supplements purchased from Lonza (EGF, fetuin, dexamethasone, and gentamicin without insulin), and supplemented with 10% fetal calf serum as previously described(23). A second growth media containing 5 ng/mL bFGF and 20% fetal calf serum was used during optimization as it was previously shown to improve expansion of myogenic cells(22). Myogenic cells were either cryopreserved in 90% growth medium with 5% fetal calf serum and 5% DMSO at passage 1 or 2 then used at passage 3-5 for the generation of myobundles or staining. A sample of primary human skeletal myoblasts from additional donor was purchased from Lonza for comparison.

For calcium imaging studies, expanded myogenic cells were transduced with a lentiviral vector encoding the fluorescent calcium reporter GCaMP6(28) driven by a myosin heavy chain-creatine kinase promoter MHCK7(29) for muscle specific expression.

For the measurements of myofiber length and nuclei number, 5% of myogenic cells used for myobundle formation were transduced with a lentiviral vector encoding MHCK7 driven GFP(44). This allowed the visualization and measurement of individual GFP^+ myotubes within myobundles using immunostaining and confocal microscopy.

Fabrication of Human Myobundles

Myobundles were formed by modifying our previously published methods for engineered rodent muscle tissues(13, 14) (Figure 1- figure supplement 2). Expanded myogenic cells were dissociated in 0.025% trypsin-EDTA to a single cell suspension and encapsulated in a fibrinogen (Akron) and matrigel (BD Biosciences) solution on laser cut Cerex® frames (9.2 x 9.5 mm outer dimensions, 6.8 x 8.3 mm inner dimensions) within PDMS molds (cast from Teflon masters and pretreated with pluronic) at $15x10^6$ cells/mL ($7.5x10^5$ cells per myobundle). Specifically, a cell solution ($7.5x10^5$ cells in 17.2 µL media per bundle + 2 µL of 50 unit/mL thrombin in 0.1% BSA in PBS (Sigma)) and a gelling solution (11 µL media + 10 µL Matrigel + 10 µL of 20 mg/mL Fibrinogen in DMEM) were prepared in separate vials on ice for up to six myobundles per vial. Gelling solution was added to the cell solution and mixed thoroughly then each bundle was individual pipetted within the PDMS mold and onto the frame. The cell/hydrogel mixture was polymerized for 30 min at 37º C followed by incubation in growth media containing 1.5 mg/mL 6-aminocaproic acid (ACA, Sigma). Myobundles were kept in growth media during gel compaction (3-5 days) and then switched to low glucose DMEM (Gibco) with 2% horse serum (Hyclone), 2 mg/mL ACA and 10 µg/mL insulin (Sigma). Frames were removed from molds at the time of switch to low serum medium and cultured dynamically in suspension for an additional 1-4 weeks. Starting from a 50 mg donor biopsy, typical cell expansion for 5 passages can allow generation of at least 1000 myobundles with a total mass of

>5 g, representing a >100-fold amplification of muscle mass when going from native to engineered tissue system.

All drugs were purchased from Sigma. Clenbuterol hydrochloride, chloroquine phosphate, and cerivastatin sodium salt hydrate were prepared at 1000X stock solutions in PBS (control) and sterile-filtered for use. Lovastatin was prepared as a 10,000X stock solution in DMSO in which case DMSO was used as vehicle control. Drugs studies in myobundles or 2D cultures were initiated after one week of differentiation. Myobundles were replenished with fresh media and drug each day to maintain drug concentration.

Measurement of Contractile Force

Electrically or chemically stimulated contractile force generation in myobundles was measured using a custom force measurement set-up as previously described(13, 14). Briefly, single myobundles on a frame were transferred to the bath of the force measurement set-up, maintained at 37 ºC. One end of the bundle was secured by a pin to an immobile PDMS block and the other end was attached to a PDMS float connected to the force transducer mounted on a computer-controlled motorized linear actuator (Thor Labs). The sides of the frame were cut to allow myobundle stretch by the actuator and isometric measurement of contractile force. Initially, the myobundle was set to its baseline length using the motorized linear actuator. To assess the force-length relationship, myobundle was stretched by 2% of its culture length then stimulated by a 40V/cm, 10 ms electrical pulse using a pair of platinum electrodes and the twitch force was recorded. At 12% stretch, 1 second long stimulations at 5, 10, and 20 Hz were applied and the subsequent contractile force was recorded to assess the force-frequency relationship. Contractile force traces were analyzed for peak twitch or tetanus force, time to peak twitch, and half relaxation time using a custom MATLAB program. For studies with acetylcholine, 60 µL of drug solution was added to the 6 mL bath at t = 5 sec of recording.

Imaging of Calcium Transients

Myobundles expressing the MHCK7-GcaMP6 reporter were non-destructively monitored for calcium transients following differentiation. A live imaging chamber with heated enclosure was used to maintain cells in physiological conditions during recording. Bundles were placed in sterile tyrode's solution in a custom-designed glass-bottom bath containing electrodes for stimulation. Video-images were acquired using an Andor iXon camera affixed to a Nikon microscope with a FITC filter and either 4x or 10x objective. During studies with caffeine and acetylcholine, 60 µL of drug solution was added to the bath at t = 5 sec of recording. Video was analyzed using Andor Solis software and relative changes in fluorescence signal were calculated by ΔF/F = (Peak-Trough) / (Trough-Background) as previously described(14).

Immunohistochemistry

Cells were fixed in 4% paraformaldehyde in PBS for 10 minutes and myobundles were fixed in 2% paraformaldehyde in PBS overnight at 4º C. Following fixation, samples were washed in PBS then blocked in 5% chick serum with 0.2% Triton-X 100. The following primary antibodies were used for tissue characterization: desmin (SCBT, 1:200), anti-GFP (Life Technologies, 1:200), laminin (Abcam, 1:200), muscle creatine kinase (SCBT, 1:100), MyoD (BD, 1:100), myogenin (SCBT, 1:100), myosin heavy chain 1/2/4/6 (SCBT, 1:100), Pax7 (DSHB, 1:50), sarcomeric α-actinin (Sigma, 1:200), and vimentin (Sigma, 1:200). Corresponding fluorescently labeled secondary antibodies (1:200), α-bungarotoxin (1:100), and phalloidin (1:200) were purchased from Life Technologies. Oil Red O staining was performed using standard protocols on cryosections of myobundles fixed in 4% paraformaldehyde. Hematoxylin and eosin stain was performed on paraffin embedded sections of 2% paraformaldehyde fixed myobundles using Harris modified hematoxylin (Sigma) and Eosin Y (Sigma). Images were acquired using a Zeiss 510 inverted confocal microscope and analyzed using LSM Image Software. Mosaic images for fiber length measurements were generated using Mosaic J in FIJI.

Western Blotting

Cell or myobundle protein was isolated in RIPA lysis and extraction buffer with protease inhibitor (Sigma). Protein concentration was determined using BCA assay (Pierce) according to manufacturer's instructions. Western blot was performed using Bio- RadMini-PROTEAN gels and the Mini-PROTEAN Tetra cell, Mini Trans-blot module. The following primary antibodies were used for detection: GAPDH (SCBT, 1:500), LC3 (Cell Signaling, 1:200), muscle creatine kinase (SCBT, 1:200), myosin heavy chain 1/2/4/6 (SCBT, 1:200), and sarcomeric alpha-actinin (Sigma, 1:200). HRP conjugated anti-mouse (1:20,000) and anti-goat (1:5000) antibody were purchased from Sigma, and HRP conjugated anti-rabbit was purchased from SCBT (1:5000). Chemiluminescence was performed using Clarity Western ECL substrate (Bio-Rad). Images were acquired using a Bio-Rad Chemidoc and analyzed using ImageJ.

Statistics

Results are presents as mean ± SD. Statistical significance was determined by unpaired t-test or one-way ANOVA with post-hoc Bonferroni-Holm test. $P<0.05$ was considered statistically significant.

ACKNOWLEDGEMENTS

We are grateful to Dr. Edward Smith and Dr. Robert Lark for providing muscle biopsies.

REFERENCES

1. Dambach DM, Uppal H. Improving Risk Assessment. Sci Transl Med. 2012;4(159):159ps22.
2. Bhatia SN, Ingber DE. Microfluidic organs-on-chips. Nature biotechnology. 2014;32(8):760-72.
3. Pedersen BK, Febbraio MA. Muscles, exercise and obesity: skeletal muscle as a secretory organ. Nature reviews Endocrinology. 2012;8(8):457-65.
4. von Keutz E, Schluter G. Preclinical safety evaluation of cerivastatin, a novel HMG-CoA reductase inhibitor. The American journal of cardiology. 1998;82(4b):11j-7j.
5. Thompson PD, Clarkson PM, Rosenson RS. An assessment of statin safety by muscle experts. The American journal of cardiology. 2006;97(8a):69c-76c.
6. Blau HM, Webster C. Isolation and characterization of human muscle cells. Proceedings of the National Academy of Sciences of the United States of America. 1981;78(9):5623-7.
7. Guo X, Greene K, Akanda N, Smith A, Stancescu M, Lambert S, et al. In vitro Differentiation of Functional Human Skeletal Myotubes in a Defined System. Biomaterials science. 2014;2(1):131-8.
8. Eberli D, Soker S, Atala A, Yoo JJ. Optimization of human skeletal muscle precursor cell culture and myofiber formation in vitro. Methods (San Diego, Calif). 2009;47(2):98-103.
9. Smith AS, Long CJ, Pirozzi K, Najjar S, McAleer C, Vandenburgh HH, et al. A multiplexed chip-based assay system for investigating the functional development of human skeletal myotubes in vitro. Journal of biotechnology. 2014;185c:15-8.
10. Ciciliot S, Rossi AC, Dyar KA, Blaauw B, Schiaffino S. Muscle type and fiber type specificity in muscle wasting. The international journal of biochemistry & cell biology. 2013;45(10):2191-9.
11. Dennis RG, Kosnik PE, 2nd. Excitability and isometric contractile properties of mammalian skeletal muscle constructs engineered in vitro. In vitro cellular & developmental biology Animal. 2000;36(5):327-35.
12. Huang YC, Dennis RG, Larkin L, Baar K. Rapid formation of functional muscle in vitro using fibrin gels. Journal of applied physiology (Bethesda, Md : 1985). 2005;98(2):706-13.
13. Hinds S, Bian W, Dennis RG, Bursac N. The role of extracellular matrix composition in structure and function of bioengineered skeletal muscle. Biomaterials. 2011;32(14):3575-83.
14. Juhas M, Engelmayr GC, Jr., Fontanella AN, Palmer GM, Bursac N. Biomimetic engineered muscle with capacity for vascular integration and functional maturation in vivo. Proceedings of the National Academy of Sciences of the United States of America. 2014;111(15):5508-13.
15. Vandenburgh H, Shansky J, Benesch-Lee F, Barbata V, Reid J, Thorrez L, et al. Drug-screening platform based on the contractility of tissue-engineered muscle. Muscle & nerve. 2008;37(4):438-47.
16. Lee PH, Vandenburgh HH. Skeletal muscle atrophy in bioengineered skeletal muscle: a new model system. Tissue engineering Part A. 2013;19(19-20):2147-55.
17. Moon du G, Christ G, Stitzel JD, Atala A, Yoo JJ. Cyclic mechanical preconditioning improves engineered muscle contraction. Tissue engineering Part A. 2008;14(4):473-82.
18. Mudera V, Smith AS, Brady MA, Lewis MP. The effect of cell density on the maturation and contractile ability of muscle derived cells in a 3D tissue-engineered skeletal muscle model and determination of the cellular and mechanical stimuli required for the synthesis of a postural phenotype. Journal of cellular physiology. 2010;225(3):646-53.
19. Powell CA, Smiley BL, Mills J, Vandenburgh HH. Mechanical stimulation improves tissue-engineered human skeletal muscle. American journal of physiology Cell physiology. 2002;283(5):C1557-65.
20. Bottinelli R, Reggiani C. Human skeletal muscle fibres: molecular and functional diversity. Progress in biophysics and molecular biology. 2000;73(2-4):195-262.
21. Fuglevand AJ, Macefield VG, Bigland-Ritchie B. Force-frequency and fatigue properties of motor units in muscles that control digits of the human hand. Journal of neurophysiology. 1999;81(4):1718-29.

22. Ham RG, St Clair JA, Webster C, Blau HM. Improved media for normal human muscle satellite cells: serum-free clonal growth and enhanced growth with low serum. In vitro cellular & developmental biology : journal of the Tissue Culture Association. 1988;24(8):833-44.
23. Cheng CS, El-Abd Y, Bui K, Hyun YE, Hughes RH, Kraus WE, et al. Conditions that promote primary human skeletal myoblast culture and muscle differentiation in vitro. American journal of physiology Cell physiology. 2014;306(4):C385-95.
24. Rassier DE, MacIntosh BR, Herzog W. Length dependence of active force production in skeletal muscle. Journal of applied physiology (Bethesda, Md : 1985). 1999;86(5):1445-57.
25. Racca AW, Beck AE, Rao VS, Flint GV, Lundy SD, Born DE, et al. Contractility and kinetics of human fetal and human adult skeletal muscle. The Journal of physiology. 2013;591(Pt 12):3049-61.
26. Cheng CS, Davis BN, Madden L, Bursac N, Truskey GA. Physiology and metabolism of tissue-engineered skeletal muscle. Experimental biology and medicine (Maywood, NJ). 2014.
27. Berchtold MW, Brinkmeier H, Muntener M. Calcium ion in skeletal muscle: its crucial role for muscle function, plasticity, and disease. Physiological reviews. 2000;80(3):1215-65.
28. Chen TW, Wardill TJ, Sun Y, Pulver SR, Renninger SL, Baohan A, et al. Ultrasensitive fluorescent proteins for imaging neuronal activity. Nature. 2013;499(7458):295-300.
29. Salva MZ, Himeda CL, Tai PW, Nishiuchi E, Gregorevic P, Allen JM, et al. Design of tissue-specific regulatory cassettes for high-level rAAV-mediated expression in skeletal and cardiac muscle. Molecular therapy : the journal of the American Society of Gene Therapy. 2007;15(2):320-9.
30. Moulds RF, Denborough MA. A study of the action of caffeine, halothane, potassium chloride and procaine on normal human skeletal muscle. Clinical and experimental pharmacology & physiology. 1974;1(3):197-209.
31. Kalamida D, Poulas K, Avramopoulou V, Fostieri E, Lagoumintzis G, Lazaridis K, et al. Muscle and neuronal nicotinic acetylcholine receptors. Structure, function and pathogenicity. The FEBS journal. 2007;274(15):3799-845.
32. Secher NH, Rube N, Secher O. Effect of tubocurarine on human soleus and gastrocnemius muscles. Acta anaesthesiologica Scandinavica. 1982;26(3):231-4.
33. Dobkin BH. Underappreciated statin-induced myopathic weakness causes disability. Neurorehabilitation and neural repair. 2005;19(3):259-63.
34. Shitara Y, Sugiyama Y. Pharmacokinetic and pharmacodynamic alterations of 3-hydroxy-3-methylglutaryl coenzyme A (HMG-CoA) reductase inhibitors: drug-drug interactions and interindividual differences in transporter and metabolic enzyme functions. Pharmacology & therapeutics. 2006;112(1):71-105.
35. Kantola T, Kivisto KT, Neuvonen PJ. Grapefruit juice greatly increases serum concentrations of lovastatin and lovastatin acid. Clinical pharmacology and therapeutics. 1998;63(4):397-402.
36. Shintani T, Klionsky DJ. Autophagy in health and disease: a double-edged sword. Science (New York, NY). 2004;306(5698):990-5.
37. Lee HS, Daniels BH, Salas E, Bollen AW, Debnath J, Margeta M. Clinical utility of LC3 and p62 immunohistochemistry in diagnosis of drug-induced autophagic vacuolar myopathies: a case-control study. PloS one. 2012;7(4):e36221.
38. Burniston JG, Clark WA, Tan LB, Goldspink DF. Dose-dependent separation of the hypertrophic and myotoxic effects of the beta(2)-adrenergic receptor agonist clenbuterol in rat striated muscles. Muscle & nerve. 2006;33(5):655-63.
39. Ryall JG, Lynch GS. The potential and the pitfalls of beta-adrenoceptor agonists for the management of skeletal muscle wasting. Pharmacology & therapeutics. 2008;120(3):219-32.
40. Chen KD, Alway SE. A physiological level of clenbuterol does not prevent atrophy or loss of force in skeletal muscle of old rats. Journal of applied physiology (Bethesda, Md : 1985). 2000;89(2):606-12.

41. Bowes J, Brown AJ, Hamon J, Jarolimek W, Sridhar A, Waldron G, et al. Reducing safety-related drug attrition: the use of in vitro pharmacological profiling. Nat Rev Drug Discov. 2012;11(12):909-22.
42. Juhas M, Bursac N. Roles of adherent myogenic cells and dynamic culture in engineered muscle function and maintenance of satellite cells. Biomaterials. 2014;35(35):9438-46.
43. Kleinstreuer NC, Yang J, Berg EL, Knudsen TB, Richard AM, Martin MT, et al. Phenotypic screening of the ToxCast chemical library to classify toxic and therapeutic mechanisms. Nature biotechnology. 2014;32(6):583-91.
44. Li M, Dickinson CE, Finkelstein EB, Neville CM, Sundback CA. The role of fibroblasts in self-assembled skeletal muscle. Tissue engineering Part A. 2011;17(21-22):2641-50.

FIGURE LEGENDS

Figure 1. Structure and cellular composition of myobundles.

(*A*) Human myogenic precursors were cast within a fibrin/matrigel matrix in PDMS molds and anchored to nylon frames. Once compacted, frames with myobundles were removed for free-floating culture. (*B*) F-actin$^+$ myofibers shown within 2-week myobundles are aligned and surrounded by laminin. (*C*) Transverse myobundle cross-section showing dense, uniformly distributed myosin heavy chain (MYH) expressing myofibers. (*D-F*) Aligned myofibers within myobundle show striated pattern of the contractile protein sarcomeric α-actinin (SAA) (*D*), myogenin (MyoG) positive nuclei (*E*), and bungarotoxin-labeled acetylcholine receptors (AChR) (*F*). (*G*) Pax7$^+$ cells (arrows) are found abutting myofibers suggesting regenerative potential. (*H*) Myofiber diameter increases with time in culture, with significant enhancement at 3 and 4 weeks versus 1 week (*, $p<0.05$, N=4 donors, n> 10 myofibers per myobundle). (*I*) Structural maturation is also evident from increased expression of muscle markers MYH, SAA, and muscle creatine kinase (MCK). Scale bars: (*B-F*) scale = 50 μm, (*G*) scale = 25 μm.

Figure 2. Contractile function of myobundles.

(*A*) Representative contractile force traces of a 3-week myobundle showing fusion of individual twitches into a stronger tetanic contraction induced by increased stimulation frequency. (*B*) Representative increase in both contractile (active) force and passive tension with increase in myobundle length for one donor at 3 weeks in culture (n=3 myobundles). (*C*) Twitch and tetanus

forces increase over time in culture with significant enhancement at 4 weeks versus 1 week (*, $p<0.05$, n=4 myobundles). (*D*) Kinetics of twitch rise and relaxation do not vary over 4 weeks in culture (n=4 myobundles). (*E*) Specific twitch and tetanus force and tetanus-to-twitch ratio for different cell sources (D1-D9, donors 1-9; CS, commercial source, Lonza). (*F*) Kinetics of twitch response for different cell sources.

Figure 3. Calcium handling of myobundles.

(*A*) Myofiber-specific expression of GCaMP6 in lentivirally transduced myobundles. SAA, sarcomeric α-actinin (scale bar = 50 μm). (*B*) Time course of GCaMP6 fluorescence during a single electrically stimulated twitch (scale bar = 200 μm) . (*C*) Representative fluorescence traces from 1 Hz and 10 Hz stimulations of 2-week old myobundles. (*D*) Amplitude of electrically stimulated calcium transient increases with time of culture and myobundle maturation (*, $p<0.05$ vs. 1 week, n=4 myobundles). (*E*) Representative fluorescence trace of acetylcholine (ACh, 100 mM bolus) stimulated calcium release in a 2-week myobundle. (*F*) ACh receptor blocker tubocurarine (25 μM) specifically and significantly reduces ACh induced calcium release without affecting electrically stimulated calcium transients (*, $p<0.05$, n=5 myobundles). Note that amplitude of Ach-induced calcium release is similar to that of calcium transient induced by tetanic (10 Hz) electrical stimulation.

Figure 4. Pharmacological validation of myobundles.

(*A-B*) Two-week application of cerivastatin (*A*) and lovastatin (*B*) at increasing doses significantly reduced tetanus force, normalized to untreated or vehicle treated (DMSO for Lovastatin) control (n=4 myobundles per donor). (*C*) Accumulation of lipids in myobundles, evaluated by Oil Red O stain, was absent from controls, moderate at lower concentrations, and considerable at higher concentrations of both statins (scale bar = 50 μm). (*D-F*) One-week exposure of myobundles to chloroquine resulted in dose-dependent decrease of contractile

force (n=4 myobundles per donor) (*D*) as well as increased expression of the autophagic pathway marker LC3B-II and decreased expression of contractile protein sarcomeric α-actinin (SAA) (E-F, n=4 myobundles per donor). (*A-F*) (*, $p<0.05$ vs. 0 μM, #, $p<0.05$ vs. all other concentrations). (*G*) Acute (thirty-minute) and (*H*) chronic (two-week) application of clenbuterol to myobundles (shown in different donors) results in a dose-dependent increase in contractile force with peak effects observed at 1 μM (acute) and 0.1 μM (chronic) and significant reduction in force generation observed at 100 μM (acute, n=3 myobundles; chronic, n=4 myobundles). (*I*) Chronic administration of 0.1 μM Clenbuterol induced hypertrophy of myofibers as evident from a rightward shift in their diameter distribution and significant increase in the average myofiber diameter (untreated, 15.7±0.3 μm vs 0.1 μM clenbuterol, 17.1±0.6 μm, *, $p<0.05$, $n \geq 55$ myofibers per myobundle, pooled for 3 myobundles).

VIDEO LEGENDS

Video 1. Spontaneous contractions of human myobundles.

Following three to five days of differentiation within the hydrogel construct, myofibers began spontaneously contracting. These contractions typically last for a few days, and are rarely seen beyond two weeks following differentiation. Video is shown in real time for 26 sec duration and at field of view of 2x1.5 mm then 0.8x0.6 mm.

Video 2. Stimulated contractions of human myobundles. Myobundles respond to electrical stimulation by forceful contraction. Here, a myobundle pair is contracting in concert with 1 Hz electrical stimulation with enough force to bend the frame on which it is attached. Video is shown in real time for 17 sec duration and at field of view of 25x25 mm.

Video 3. GCaMP6 reported calcium release of human myobundles. Myobundles formed using myogenic precursors that were lentivirally transduced with a GCaMP6 calcium reporter contain

myofibers that produce fluorescence signal in response to calcium release. Here, myobundles show calcium release in response to both twitch (1 Hz) and tetanus (10 Hz) electrical stimulation. Video is shown in real time for 36 sec duration and at field of view of 500x500 μm.

Video 4. Caffeine induced calcium release in human myobundles. Similar to human skeletal muscle, application of caffeine to myobundles induces calcium release via the ryanodine receptors. This lease to an increase in fluorescence from the GCaMP calcium reporter. Video is shown in real time for 66 sec duration and at field of view of 2x2 mm.

Video 5. Acetylcholine induced calcium release from human myobundles. Function of myobundle acetylcholine receptors was confirmed by GCaMP6 detected calcium release in response to a bolus of 10 mM acetylcholine. Myobundle response to acetylcoline was significantly blocked by the muscle relaxant tubocurarine similar to that observed clinically in human skeletal muscle. Video is shown in real time for 75 sec duration and at field of view of 2x2 mm.

SUPPLEMENTARY FIGURE LEGENDS

Figure 1 – figure supplement 1. Myogenicity of donor cells during expansion. (A) Expanded donor cells at passage three still express the muscle precursor markers desmin and (B) MyoD. (C) After switch to low serum media in 2D, myogenic cells fuse into myotubes and express myogenin (MyoG) and sarcomeric alpha-actinin (SAA). Scale bars: (A) 50 μm, (B-C) 200 μm.

Figure 1 – figure supplement 2. Schematic of myobundle fabrication. (A) Machined teflon masters were used to generate multiple replicas of PDMS molds. The PDMS molds contain an

outer ridge that fit laser-cut frames made of porous Cerex® material. (B) Separate solutions containing myogenic cells and hydrogel proteins were prepared on ice and mixed immediately prior to pipetting into the PDMS mold with frame. (C) Images depicting the appearance of the myobundles during the course of culture. At far left, the cell/hydrogel solution is gelled at 37^{o}C in a tissue culture incubator for 30 min. Following gelation, culture media is added to the well. Within 4 days, the myobundles compact and the edges come away from the PDMS mold. The compacted myobundles are removed from the mold and cultured free-floating. Scale bar = 5 mm.

Figure 1 – figure supplement 3. Characterization of myobundle architecture.

(A) Representative composite image of a myobundle consisting of aligned, F-actin^{+} myofibers surrounded by a layer of vimentin^{+} fibroblasts on the outer surface. (B, C) Hematoxylin and eosin stain at lower (B) and higher (C) magnification show uniform density of aligned, multinucleated myofibers at 3 weeks of culture. (D) F-actin^{+} immunostaining shows increased myofiber diameter with time in culture. Scale bars: (A) 500 μm, (B) 200 μm (C,D) = 50 μm.

Figure 1 – figure supplement 4. Characterization of myofiber length and myonuclei number.

(A) Representative composite image of a 3-week differentiated myobundle formed using 5% GFP expressing myogenic cells to visualize individual myofibers. Scale bar = 500 μm. (B) The average length of GFP^{+} myofibers as a function of differentiation time (20-50 myofibers per bundle, n=4-6 myobundles per time point). (C) Histogram of myonuclei number per GFP^{+} myofiber in 3-week myobundles with average and median myonuclei numbers of 7±3.6 and 6, respectively (n=127 myofibers from 6 myobundles).

Figure 2 – figure supplement 1. Optimization of myogenic cell expansion using two different media.

(A) Myogenic cells expanded in the two different media containing either bFGF or EGF had similar fractions of $MyoD^+$ cells. (B) Upon differentiation in 2D culture, these cells expressed similar levels of myogenin (n=3 coverslips) (C) Cells expanded in EGF containing media formed myobundles with significantly higher levels of contractile force than those expanded in bFGF containing media. (N=2 donors, n=4 myobundles, *, $p<0.05$)

Figure 2 – figure supplement 2. Force-frequency relationship of myobundles.

Contractile force increases with stimulation frequency. (n=4 myobundles; *, $p<0.05$ vs. 1 Hz; #, $p<0.05$ vs. 1 Hz and 5 Hz)

Figure 3 – figure supplement 1. Correlation of contractile force and calcium transients.

Each point represents a single bundle calcium transient plotted against the corresponding force, either twitch or tetanus (at 10 Hz). Data was obtained from myobundles during 4 weeks in culture prepared from the same pool of MHCK7-GCaMP6 transduced myogenic precursors.

Figure 3 – figure supplement 2. Caffeine induced calcium transients.

(A) A bolus of caffeine of different concentrations was added to the bath during video imaging and resulted in an increase in relative fluorescence amplitude ($\Delta F/F$). (B) $\Delta F/F$ at 30 seconds following caffeine administration was calculated and positively correlated with caffeine concentration. (Donor A, n=3 myobundles; Donor B n=4 myobundles; *, $p < 0.05$ vs. 20 mM)

Figure 3 – figure supplement 3. Myobundle response to acetylcholine.

(A) Myobundles exhibited a similar amplitude of calcium release in response to acetylcholine (Ach) throughout four weeks in culture. (n=4) (B) Representative trace of contractile force for a 3-week myobundle in response to a bolus of acetylcholine. (C) The amplitude of acetylcholine induced contractile force was similar to that induced by tetanic electrical stimulation. Incubation of myobundles with the ACh receptor blocker tubocurarine reduced acetylcholine induced contractile force without affecting electrically stimulated contraction at 3 weeks in culture. (n=5, *, $p<0.05$) (D) Amplitudes of calcium and contractile force responses to ACh are similar to those during tetanic electrical stimulation in myobundles from different donors. (A, n=5 myobundles; B, n=3 myobundles)

Figure 4 – figure supplement 1. Biochemical responses of human 2D myotube and 3D myobundle cultures to chloroquine. Human myogenic cells from a single donor were differentiated on 2D Matrigel coated dishes (black) or in 3D myobundles (white) then treated for one week with varying doses of chloroquine. The biochemical response of 2D and 3D muscle models were evaluated by western blot (A) and shown to be similar for (B) the dose-depended accumulation of LC3B-II and the reduction of contractile proteins (C) sarcomeric alpha actinin (SAA) and (D) myosin heavy chain (MYH) (n=4 2D wells or myobundles, #, $p<0.05$ vs. control and 1 μM).

Figure 4 – figure supplement 2. Improved myobundle function following clenbuterol treatment.

(A) Clenbuterol-induced increase in force was reproduced among multiple donors following two week treatment (n=4 myobundles per donor, *, $p<0.05$). Dose response for donor A is shown in Figure 4H. (B) Clenbuterol increased myofiber diameter, visualized by F-actin staining. Scale bar = 100 μm. Quantification of these immunostainings is shown in Figure 4I.

Source Code file contains custom MATLAB code used in this study.

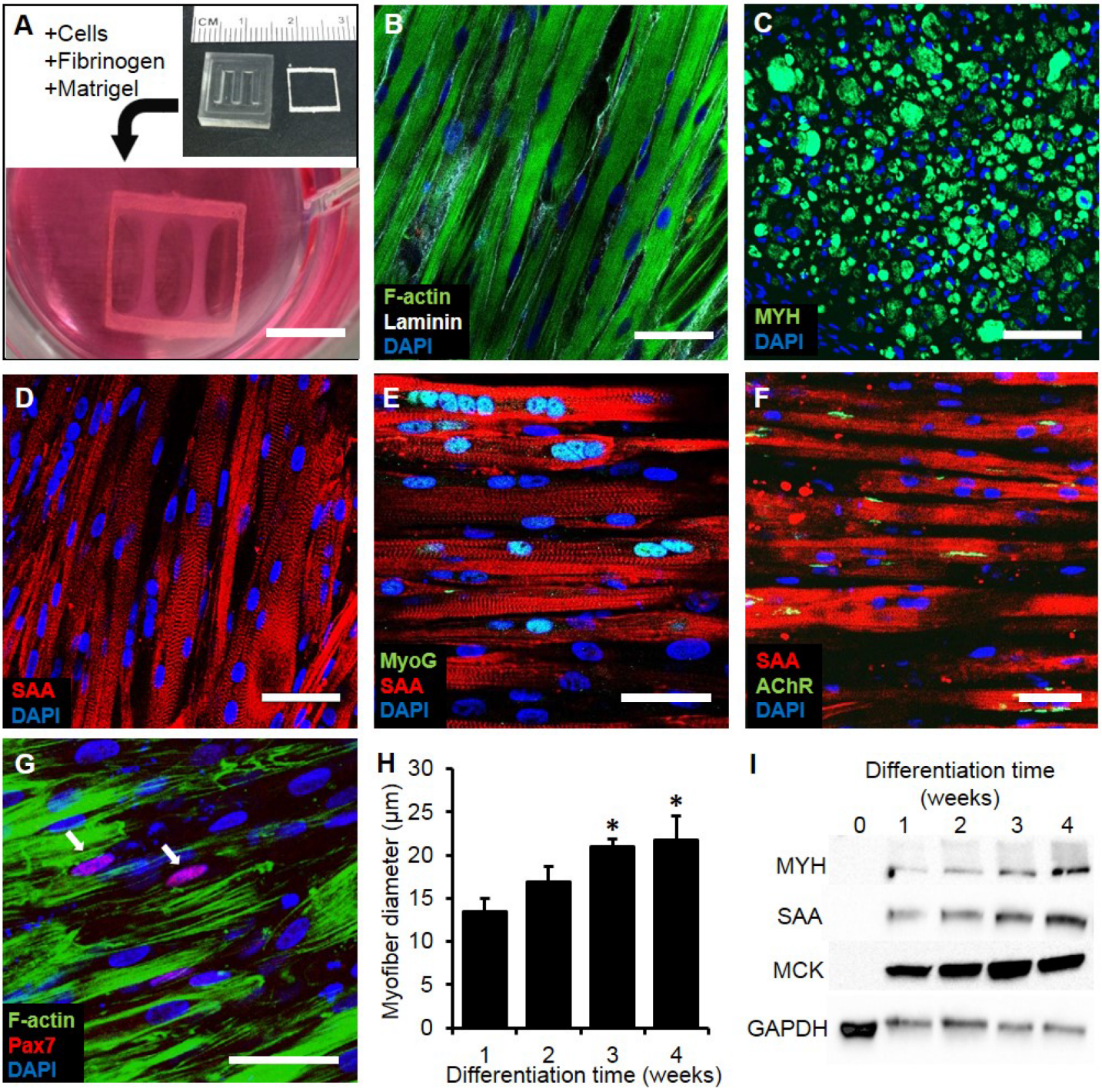
A
+Cells
+Fibrinogen
+Matrigel
B
F-actin
Laminin
DAPI
C
MYH
DAPI
D
SAA
DAPI
E
MyoG
SAA
DAPI
F
SAA
AChR
DAPI
G
F-actin
Pax7
DAPI
H
Myofiber diameter (μm)
0
5
10
15
20
25
30
*
*
1
2
3
4
Differentiation time (weeks)
I
Differentiation time (weeks)
0
1
2
3
4
MYH
SAA
MCK
GAPDH

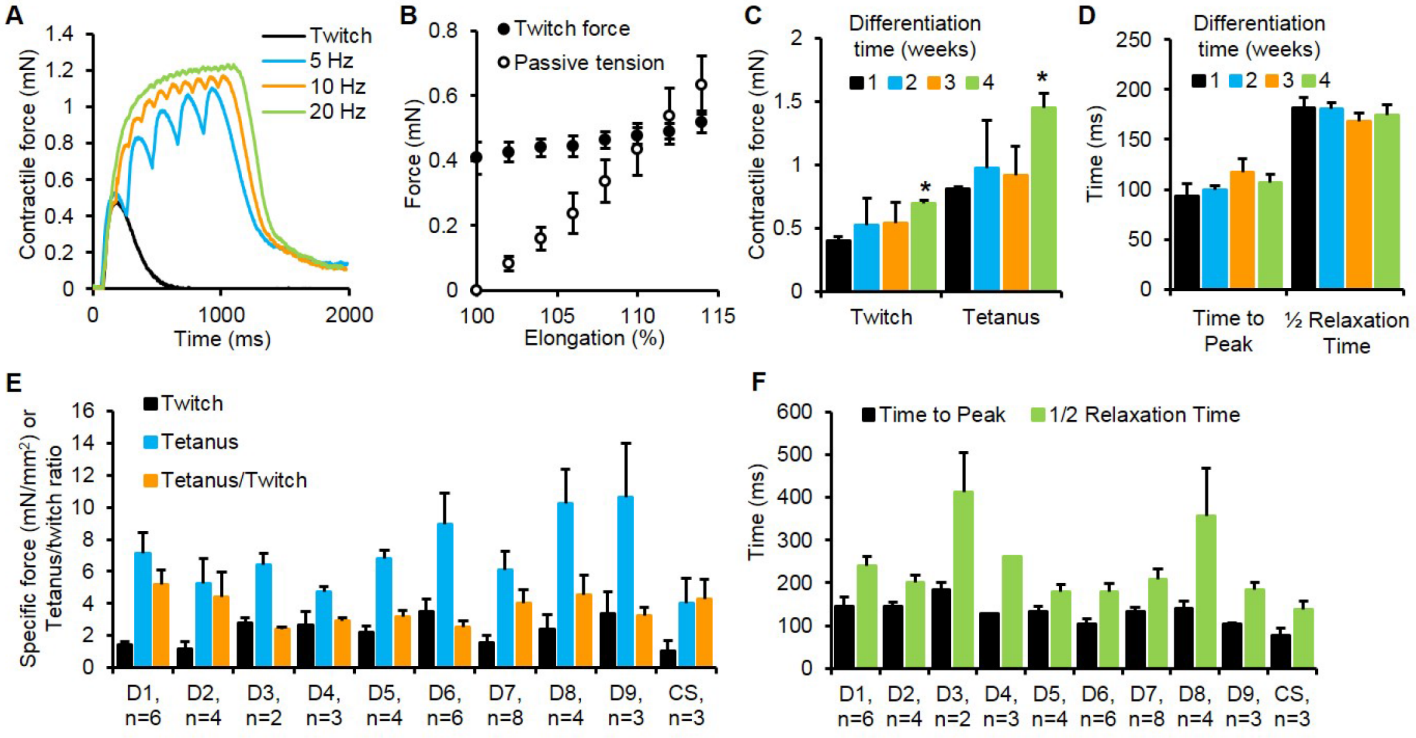
A
Contractile force (mN)
Time (ms)
Twitch
5 Hz
10 Hz
20 Hz
B
Force (mN)
Elongation (%)
Twitch force
Passive tension
C
Contractile force (mN)
Differentiation time (weeks)
1 2 3 4
Twitch
Tetanus
D
Time (ms)
Differentiation time (weeks)
1 2 3 4
Time to Peak
½ Relaxation Time
E
Specific force (mN/mm²) or Tetanus/twitch ratio
Twitch
Tetanus
Tetanus/Twitch
D1, n=6
D2, n=4
D3, n=2
D4, n=3
D5, n=4
D6, n=6
D7, n=8
D8, n=4
D9, n=3
CS, n=3
F
Time (ms)
Time to Peak
1/2 Relaxation Time
D1, n=6
D2, n=4
D3, n=2
D4, n=3
D5, n=4
D6, n=6
D7, n=8
D8, n=4
D9, n=3
CS, n=3

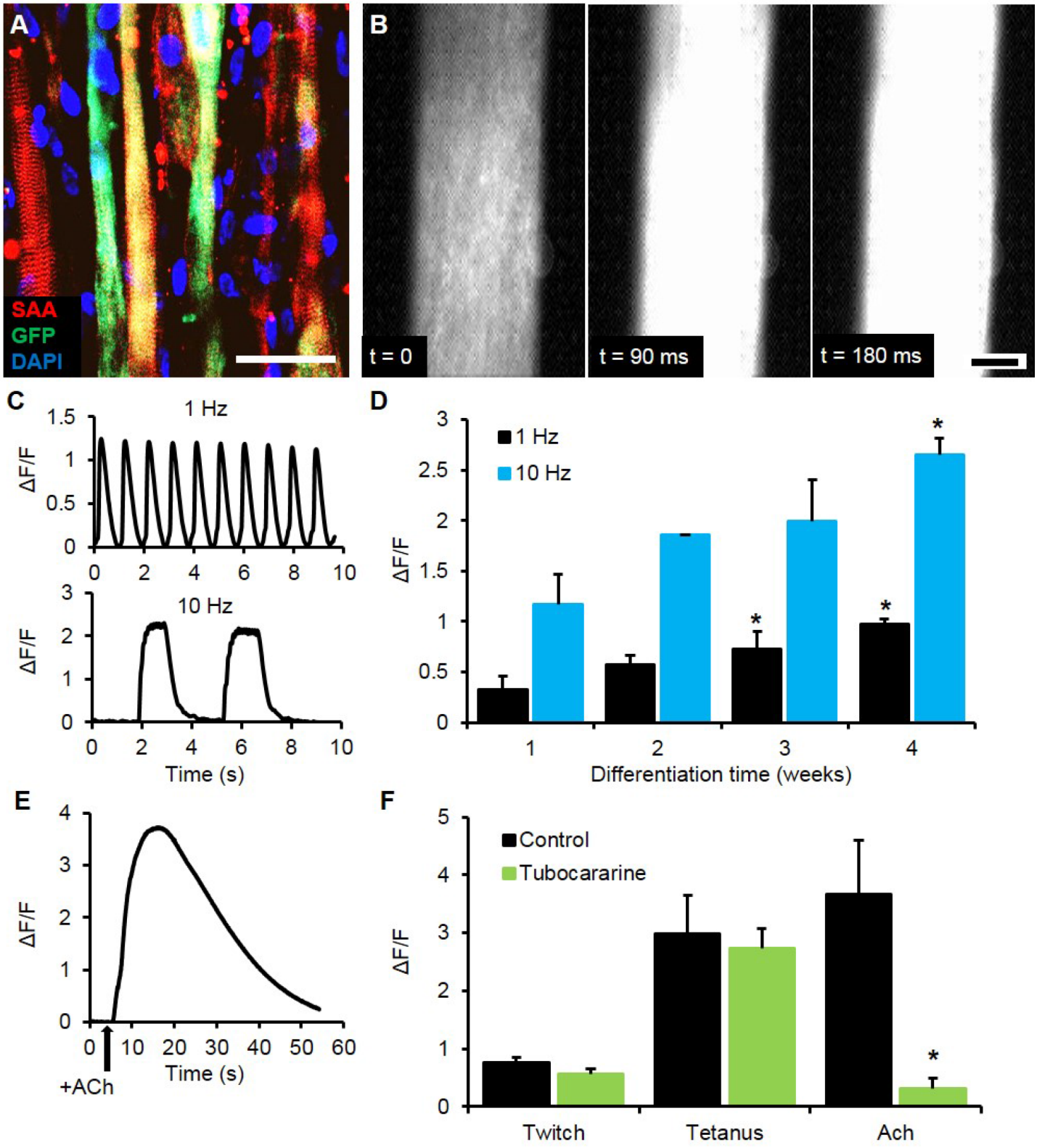
A
SAA
GFP
DAPI
B
t = 0
t = 90 ms
t = 180 ms
C
1 Hz
ΔF/F
10 Hz
Time (s)
D
1 Hz
10 Hz
ΔF/F
Differentiation time (weeks)
E
ΔF/F
+ACh
Time (s)
F
Control
Tubocararine
ΔF/F
Twitch
Tetanus
Ach

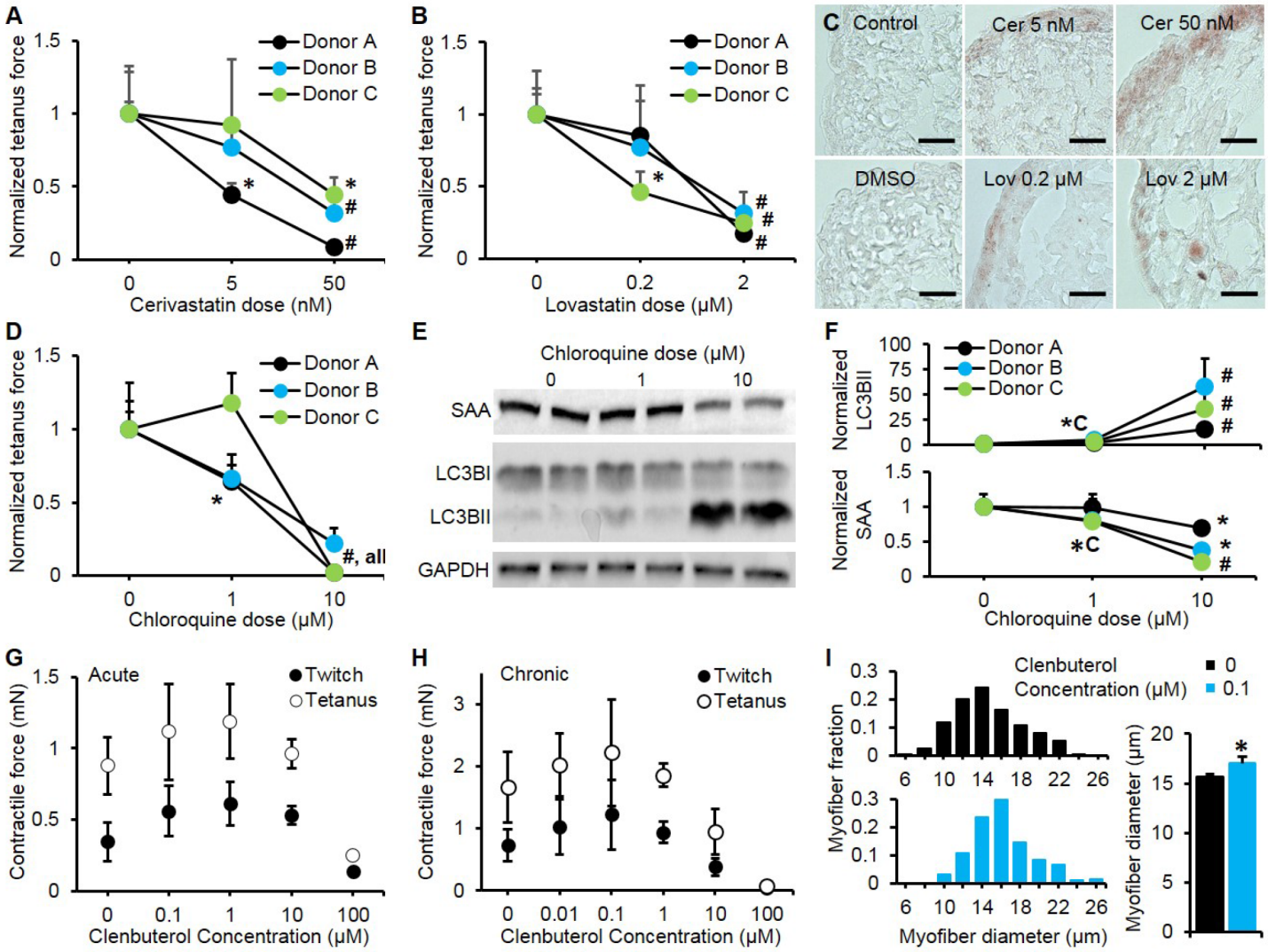
A
Normalized tetanus force
Donor A
Donor B
Donor C
Cerivastatin dose (nM)
B
Lovastatin dose (μM)
C
Control
Cer 5 nM
Cer 50 nM
DMSO
Lov 0.2 μM
Lov 2 μM
D
Chloroquine dose (μM)
#, all
E
SAA
LC3BI
LC3BII
GAPDH
F
Normalized LC3BII
Normalized SAA
*C
G
Acute
Twitch
Tetanus
Contractile force (mN)
Clenbuterol Concentration (μM)
H
Chronic
I
Clenbuterol Concentration (μM)
Myofiber fraction
Myofiber diameter (μm)